

Helmholtz dark solitons

P. Chamorro-Posada

Departamento de Teoría de la Señal y Comunicaciones e Ingeniería Telemática, Universidad de Valladolid, Escuela Técnica Superior de Ingenieros de Telecomunicación, Campus Miguel Delibes s/n, 47011 Valladolid, Spain

G. S. McDonald

Joule Physics Laboratory, School of Sciences, Institute of Materials Research, University of Salford, Salford M5 4WT, UK

Received October 17, 2002

A general dark-soliton solution of the Helmholtz equation (with defocusing Kerr nonlinearity) that has on- and off-axis, gray and black, paraxial and Helmholtz solitons as particular solutions, is reported. Modifications to soliton transverse velocity, width, phase period, and existence conditions are derived and explained in geometrical terms. Simulations verify analytical predictions and also demonstrate spontaneous formation of Helmholtz solitons and transparency of their interactions. © 2003 Optical Society of America

OCIS codes: 000.2690, 190.0190, 190.3270, 190.4420, 190.5530, 190.5940.

Spatial optical solitons play a fundamental role in the dynamics of nonlinear beams,¹ and an accurate description of properties such as oblique propagation and mutual interactions is essential. Solitons that propagate at modest or large angles relative to the reference longitudinal direction, or to each other, experience a type of nonparaxiality that can be accurately described by a nonlinear Helmholtz equation (NHE). For a single soliton beam that coincides with longitudinal axis ζ , off-axis propagation results if only the axis is rotated, whereby $\partial_{\zeta\zeta}$ is no longer negligible. Moreover, the resultant NHE can describe the total electric field of both forward- and backward-propagating components and thus of soliton interactions at arbitrary angles.

Some optical contexts, such as intense self-focusing, give rise to a more general type of nonparaxiality.²⁻⁴ Paraxiality is commonly defined through a small parameter, $\kappa = w_0^2/4L_D^2$, where w_0 is the beam width,²⁻⁵ $L_D = kw_0^2/2$, and $k = n_0\omega/c$. Order-of-magnitude analysis,^{2,3} based on κ , then yields leading corrections to a paraxial wave equation. A near-paraxial beam, well described by scalar electric-field and refractive-index distributions, if it is considered in a reference frame rotated by θ , acquires an effective transverse velocity V , but the beam itself remains intrinsically scalar in character. The usual paraxial condition, $\kappa \approx 0$, is still preserved, but now $2\kappa V^2 = \tan^2 \theta$ can assume arbitrarily large values. In this Letter, the presence of this type of potentially dominant nonparaxial correction is demonstrated through exact solution of the NHE. Helmholtz-type nonparaxiality alone is shown to result in nontrivial modifications to soliton propagation characteristics.

The equivalence of the nonparaxial nonlinear Schrödinger equation and the appropriate NHE was recently noted.⁵ It permits identification of nonparaxial generalizations of conventional soliton theory as exact analytical Helmholtz bright soliton solutions.⁶ Physical interpretations⁶ and analytical properties⁷ of Helmholtz bright solitons have been described; they permit the development and testing of new nonparaxial beam propagation techniques.⁸

Here we report, for the first time to our knowledge, a general Helmholtz dark-soliton solution for a defocusing Kerr nonlinearity. The conditions for experimental achievement of optical dark solitons are well known,^{9,10} and our theoretical predictions are expected to be directly observable. To highlight the modifications to paraxial theory, we solve the equivalent defocusing nonparaxial nonlinear Schrödinger equation⁵⁻⁸:

$$\kappa \frac{\partial^2 u}{\partial \zeta^2} + i \frac{\partial u}{\partial \zeta} + \frac{1}{2} \frac{\partial^2 u}{\partial \xi^2} - |u|^2 u = 0, \quad (1)$$

where $\zeta = z/L_D$, $\xi = \sqrt{2}x/w_0$, and $u(\xi, \zeta) = (k|n_2|L_D/n_0)^{1/2}A(\xi, \zeta)$ are longitudinal and transverse coordinates and the field amplitude, respectively, in terms of Kerr coefficient n_2 , unscaled variables z and x , and field envelope A defined by $E(x, z) = A(x, z)\exp(ikz)$. For simplicity, a uniform-background field u_0 is assumed. A general dark solution of Eq. (1) is then found to be

$$\begin{aligned} u(\xi, \zeta) &= u_0(A \tanh \Theta + iF) \\ &\times \exp \left[i \left(\frac{1 - 4\kappa u_0^2}{1 + 2\kappa V^2} \right)^{1/2} \left(-V\xi + \frac{\zeta}{2\kappa} \right) \right] \\ &\times \exp \left(-i \frac{\zeta}{2\kappa} \right), \end{aligned} \quad (2)$$

where

$$\Theta = \frac{u_0 A (\xi + W\zeta)}{(1 + 2\kappa W^2)^{1/2}} \quad (3)$$

and

$$W = \frac{V - V_0}{1 + 2\kappa V V_0} \quad (4)$$

is a net transverse velocity involving V (from the choice of reference direction) and V_0 (a gray-soliton component), given by

$$V_0 = \frac{u_0 F}{[1 - (2 + F^2)2\kappa u_0^2]^{1/2}}. \quad (5)$$

F and A are real constants, where $F = \pm(1 - A^2)^{1/2}$. $F = 0$ corresponds to Helmholtz black solitons,

whereas $|F| > 0$ yields gray solitons. In the paraxial limit,⁵ the nonlinear Schrödinger equation (NLS) dark soliton^{11–13} is obtained:

$$u(\xi, \zeta) = u_0(A \tanh \Theta + iF)\exp(-iV\xi) \times \exp\left(-iu_0^2\zeta - i\frac{1}{2}V^2\zeta\right), \quad (6)$$

where

$$\Theta = u_0A[\xi + (V - Fu_0)\zeta]. \quad (7)$$

A particular Helmholtz dark-soliton solution for which $V = 0$ and $F = 0$ was reported earlier.^{14,15} Interestingly, a simple ansatz approach¹⁵ is insufficient for determining the complete general solution presented here. Instead, we have also used geometrical considerations and invariance relations for Helmholtz solutions when the axes are rotated:

$$\xi = \frac{\xi' + V\zeta'}{(1 + 2\kappa V^2)^{1/2}}, \quad \zeta = \frac{-2\kappa V\xi' + \zeta'}{(1 + 2\kappa V^2)^{1/2}},$$

$$u(\xi, \zeta) = \exp\left(i\left\{\frac{V\xi'}{(1 + 2\kappa V^2)^{1/2}} + \frac{1}{2\kappa}\left[1 - \frac{1}{(1 + 2\kappa V^2)^{1/2}}\right]\zeta'\right\}\right)u'(\xi', \zeta'), \quad (8)$$

where rotation angle θ in the unscaled coordinate system is given by $\sec \theta = (1 + 2\kappa V^2)^{1/2}$.

The phase period of Helmholtz dark solitons is governed by the longitudinal wave number that is given by two factors: $\exp(-i\zeta/2\kappa)$, which is due to the forward reference frame, and projection of the nonlinear correction factor $(1 - 4\kappa u_0^2)^{1/2}$ onto the ζ axis. The transverse velocity of paraxial dark solitons is $V - Fu_0$. However, a more accurate description involves velocity summation in the unscaled coordinate system, Eq. (4), and modifications of the intrinsic gray-soliton velocity, Eq. (5).

Nonzero W corresponds to off-axis propagation. Geometrical considerations then imply that the beam width projected onto the transverse axis should increase⁶ (a feature absent from paraxial theory, in which this width is constant). In fact, the inverse soliton width is given by

$$\xi_0^{-1} = \frac{u_0A}{(1 + 2\kappa W^2)^{1/2}}. \quad (9)$$

The beam width enlargement factor can also be written as $(1 + 2\kappa W^2)^{1/2} = \sec(\theta - \theta_0)$, where $\theta_0 = \sec^{-1}[(1 + 2\kappa V_0^2)^{1/2}]$ is the angle associated with V_0 and $\theta = \sec^{-1}[(1 + 2\kappa V^2)^{1/2}]$ is defined by choice of reference frame (see Fig. 1).

Paraxial dark solitons exist for arbitrary values of background intensity.^{11–13} Helmholtz black solitons exist only¹⁴ for $4\kappa u_0^2 < 1$, which corresponds to $|2n_2I| < n_0$, where $I = |E_0|^2$ is the unscaled background intensity, and when the size of the nonlinear phase shift is less than the linear contribution. The refractive index thus remains positive (a condition implicit in the paraxial NLS that appears explicitly

in the NHE solution). Paraxial gray solitons exist for any nonzero $|F| < 1$, whereas Helmholtz gray solitons have a more limited range of F , given by $0 < |F| < |F|_{\max} = (1 - 4\kappa u_0^2)^{1/2}/(2\kappa u_0^2)^{1/2}$, where $\theta_0 = \pm\pi/2$ for $|F| = |F|_{\max}$, revealing the physical limit imposed on the largest possible transverse velocity.

Helmholtz dark solitons can be studied by use of recently developed numerical techniques⁸; analysis⁸ uncovered intrinsic limitations of traditional approaches.¹⁴ To explore whether Helmholtz dark solitons are spontaneously created from an initial field profile that does not correspond to an exact soliton, we first consider the initial condition

$$u(\xi, 0) = u_0 \tanh(u_0 a \xi). \quad (10)$$

Parameter a controls the inverse width of the initial profile. The generation of $2N_0 + 1$ paraxial solitons is expected during evolution governed by the NLS^{11,12} (N_0 is the largest integer that satisfies $N_0 < 1/a$).

NLS and NHE simulations have been carried out for $1 \leq u_0 \leq 5$, $0 < a \leq 1$, and $\kappa = 0.001$. Figure 2

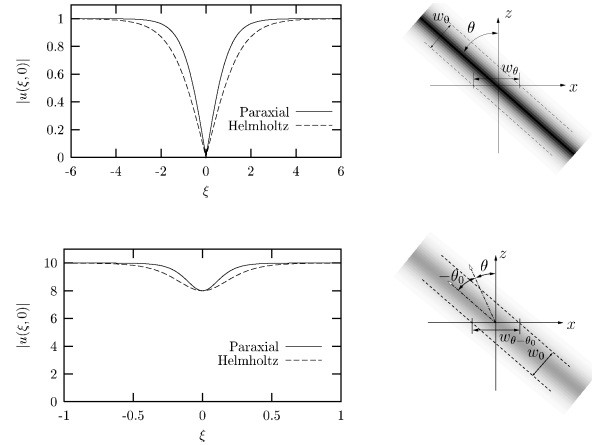


Fig. 1. Comparison of transverse profiles and geometries of paraxial and Helmholtz solitons ($\kappa = 0.001$): black solitons (top) with $V = 25$ and $u_0 = 1$. $F = 0.8$ gray solitons (bottom) with $V = 10$ and $u_0 = 10$. w_θ and $w_{\theta-\theta_0}$ are the unscaled x widths.

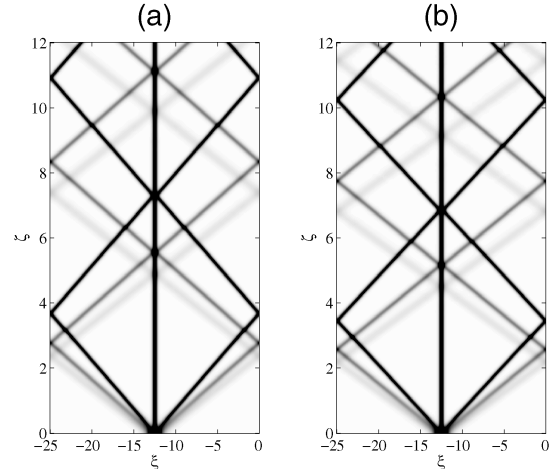


Fig. 2. Spontaneous generation and subsequent interactions of paraxial (left) and Helmholtz (right) dark solitons.

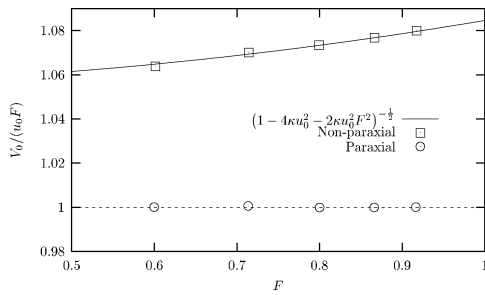


Fig. 3. Normalized transverse velocities of simulated gray solitons (symbols) and the corresponding analytical predictions (curves).

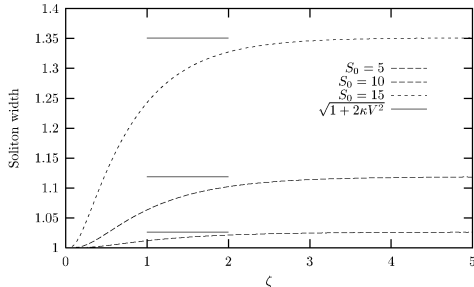


Fig. 4. Evolution of normalized beam widths (toward ξ_0) for initially perturbed off-axis Helmholtz black solitons (horizontal lines denote analytical predictions for their asymptotic values).

shows results for $a = 0.26$ and $u_0 = 5$. In general, solitons and radiation modes are created.¹⁶ Here, $1/a$ is close to, and just exceeds, an integer value, so radiation modes are of sufficiently low amplitude that only solitons are visible. Clear differences appear in the transverse velocities of the gray beams generated. In each simulation, two pairs of gray solitons are well defined, whereas the third pair has a much smaller amplitude and is almost indistinguishable from the flat background. Helmholtz dark solitons are discovered to be stable robust attractors and to possess the key property of transparent mutual interaction. Spectacular agreement is found between NHE simulations and exact analytical results. Figure 3 shows transverse velocities derived from both NLS and NHE simulations (symbols) and compares these data with the corresponding analytical predictions (solid and dashed curves).

We also consider the initial condition

$$u(\xi, 0) = u_0 \tanh(u_0 \xi) \exp(-iS_0 \xi). \quad (11)$$

In a paraxial framework, a single black soliton results that has transverse velocity S_0 . For $\kappa u_0^2 \ll 1$, the

NHE evolution can be shown to be equivalent to the propagation of an initially perturbed (reduced width) on-axis NLS black soliton. Inverse scattering techniques,¹¹⁻¹³ then, implies the generation of only one Helmholtz soliton. Figure 4 shows the evolving beam widths for $u_0 = 1$, $\kappa = 0.001$, and three values of S_0 that correspond to propagation angles of $\theta = \tan^{-1}(\sqrt{2\kappa}V) = 12.9^\circ, 26.6^\circ, 42.1^\circ$, respectively. The predicted asymptotic values of the Helmholtz beam width are given by $(1 + 2\kappa V^2)^{1/2}$, where $V = S_0/(1 - 2\kappa S_0^2)^{1/2}$ when $\kappa u_0^2 \ll 1$. Whereas similarly perturbed Helmholtz bright solitons undergo large oscillations over long propagation distances ($\xi > 50$),⁸ dark beams are found to exhibit a surprisingly fast convergence to the asymptotic solutions.

The Helmholtz solitons discussed here are likely to lead to a new class of soliton solution, modified by the same Helmholtz-type correction, appropriate to generalized nonlinearities, higher dimensions (e.g., stripes, rings, vortices), coupled modes (e.g., interactions, vector solitons) and other soliton wave equations.^{1,13}

This study was supported by the Junta de Castilla y Leon, project VA 110/02. P. Chamorro-Posada's e-mail address is pedcha@tel.uva.es.

References

1. G. I. Stegeman and M. Segev, *Science* **286**, 1518 (1999).
2. S. Chi and Q. Guo, *Opt. Lett.* **20**, 1598 (1995).
3. A. Ciattoni, P. Di Porto, B. Crosignani, and A. Yariv, *J. Opt. Soc. Am. B* **17**, 809 (2000).
4. S. Blair, *Chaos* **10**, 570 (2000).
5. P. Chamorro-Posada, G. S. McDonald, and G. H. C. New, *J. Opt. Soc. Am. B* **19**, 1216 (2002).
6. P. Chamorro-Posada, G. S. McDonald, and G. H. C. New, *J. Mod. Opt.* **45**, 1111 (1998).
7. P. Chamorro-Posada, G. S. McDonald, and G. H. C. New, *J. Mod. Opt.* **47**, 1877 (2000).
8. P. Chamorro-Posada, G. S. McDonald, and G. H. C. New, *Opt. Commun.* **19**, 1 (2001).
9. G. A. Swartzlander, Jr., D. R. Anderson, J. J. Regan, H. Yin, and A. E. Kaplan, *Phys. Rev. Lett.* **66**, 1583 (1991).
10. G. R. Allan, S. K. Skinner, D. R. Andersen, and A. L. Smirl, *Opt. Lett.* **16**, 156 (1991).
11. V. E. Zakharov and A. B. Shabat, *Zh. Eksp. Teor. Fiz.* **64**, 1627 (1973).
12. Y. S. Kivshar, *IEEE J. Quantum Electron.* **29**, 250 (1993).
13. Y. S. Kivshar and B. Luther-Davies, *Phys. Rep.* **298**, 81 (1998).
14. E. Granot, S. Sternklar, Y. Isbi, B. Malomed, and A. Lewis, *Opt. Commun.* **178**, 431 (2000).
15. T. A. Laine and A. T. Friberg, *J. Opt. Soc. Am. B* **17**, 751 (2000).
16. K. J. Blow and N. J. Doran, *Phys. Lett.* **107A**, 55 (1985).